

Engineering Long Range Distance Independent Entanglement through Kondo Impurities in Spin Chains

Abolfazl Bayat

Department of Physics and Astronomy,
University College London, Gower St.,
London WC1E 6BT, UK

Pasquale Sodano

Dipartimento di Fisica e Sezione I.N.F.N.,
Universita' di Perugia, Via A. Pascoli,
Perugia, 06123, Italy

Sougato Bose

Department of Physics and Astronomy,
University College London, Gower St.,
London WC1E 6BT, UK

We investigate the entanglement properties of the Kondo spin chain when it is prepared in its ground state as well as its dynamics following a single bond quench. We show that a true measure of entanglement such as negativity enables to characterize the unique features of the gapless Kondo regime. We determine the spatial extent of the Kondo screening cloud and propose an ansatz for the ground state in the Kondo regime accessible to this spin chain; we also demonstrate that the impurity spin is indeed maximally entangled with the Kondo cloud. We exploit these features of the entanglement in the gapless Kondo regime to show that a single local quench at one end of a Kondo spin chain may always induce a fast and long lived oscillatory dynamics, which establishes a high quality entanglement between the individual spins at the opposite ends of the chain. This entanglement is a footprint of the presence of the Kondo cloud and may be engineered so as to attain - even for very large chains- a constant high value independent of the length; in addition, it is thermally robust. To better evidence the remarkable peculiarities of the Kondo regime, we carry a parallel analysis of the entanglement properties of the Kondo spin chain model in the gapped dimerised regime where these remarkable features are absent.

1 Introduction

Kondo systems [2, 1] are expected to be very distinctive in the context of entanglement for at least two reasons: (a) Despite being “gapless”, they support the emergence of a length scale ξ [2, 1] which should be reflected in the entanglement, making it markedly different from that in the more conventional gapless models studied so far; (b) They are expected to have a more exotic *form* of entanglement than the widely studied spin-spin and complementary block entanglements. Indeed, in Kondo systems, the impurity spin is expected to be mostly entangled with only a specific block of the whole system. This is, of course, merely an intuition which needs to be quantitatively verified with a genuine measure of entanglement: this task has been accomplished in [3] where we provided the only characterization of the Kondo regime based entirely on a true measure of entanglement such as negativity [4].

The simplest Kondo model [2, 5] describes a single impurity spin interacting with the conduction electrons in a metal; the ground state is a highly nontrivial many body state in which the impurity spin is screened by conduction electrons in a large orbital of size ξ - the so called Kondo screening length. Many physical observables vary on the characteristic length scale ξ , which is a well defined function of the Kondo coupling [2]. The screening length ξ determines the spatial extent of the Kondo cloud whose signatures in physical systems have been so far a challenging problem repeatedly addressed by various

means [1, 6, 7]. As we shall detail in the following an entanglement measure enables to fully determine ξ [3] and to use its knowledge to engineer long range distance independent entanglement [8].

Recently [9], it has been pointed out that the universal low energy long distance behavior of this simple Kondo model arises also in a spin chain when a magnetic impurity is coupled to the end of a gapless Heisenberg anti-ferromagnetic $J_1 - J_2$ spin 1/2 chain. The spin chain Kondo model [9] is defined by the Hamiltonian

$$H_I = J'(J_1 \sigma_1 \cdot \sigma_2 + J_2 \sigma_1 \cdot \sigma_3) + \sum_{i=2}^{N-1} J_1 \sigma_i \cdot \sigma_{i+1} + J_2 \sum_{i=2}^{N-2} \sigma_i \cdot \sigma_{i+2}, \quad (1)$$

where $\sigma_i = (\sigma_i^x, \sigma_i^y, \sigma_i^z)$ is a vector of Pauli operators at site i , N is the total length of the chain, J_2 is the next nearest neighbor coupling and the nearest neighbor coupling J_1 is normalized to 1. The impurity spin, located at one end of the chain, is accounted for by weaker couplings to the rest of the system; in the following, see Fig. 1a, both couplings J_1 and J_2 are weakened by the same factor J' , which quantifies then the impurity strength. for $0 \leq J_2 \leq J_2^c = 0.2412$, the spin system is gapless and it supports a Kondo regime [10, 1]. For $J_2 > J_2^c$, the system enters the gapped *dimer regime*, where the ground state takes a dimerised form; at the Majumdar-Ghosh [11] point ($J_2 = 0.5$), the ground state becomes just a tensor product of singlets. For $J_2 > 0.5$, incommensurability effects [12] emerge.

In the following we detail our analysis [3, 8] of the remarkable features of entanglement in the Kondo regime [2, 1] of the spin chain Kondo model. First of all, we use negativity [4] to characterize [3] the entanglement in the Kondo regime; namely, for this spin chain in the Kondo regime: (i) we demonstrate that the impurity spin is maximally entangled with the Kondo cloud; (ii) we determine the spatial extent of the Kondo screening length ξ using only an entanglement measure; (iii) we motivate an ansatz for the ground state in the Kondo regime; (iv) we evidence the scaling of negativity as pertinent parameters are varied. Then, we use the knowledge acquired in [3] to engineer- for chains of arbitrary size N - a long range distance-independent entanglement through a non-perturbative dynamical mechanism which requires only a *minimal action* on a spin chain, namely a sudden quench of a single bond [8]. The ensuing long range distance independent entanglement- as well as the remarkable entanglement oscillations observed in our numerical simulations [8]- are a footprint of the emergence of the length scale ξ in an -otherwise gapless- system. To accomplish these tasks we designed [3] a Density Matrix Renormalization Group (DMRG) approach enabling to investigate the entanglement between a single spin and a pertinent block of the chain. We also developed [8] a time dependent DMRG to simulate the dynamics of the system after a sudden quench of a local bond; to better evidence the unique properties of the entanglement in the Kondo regime we carried a parallel analysis of the entanglement properties of this model in the gapped dimerised regime where all these remarkable features of entanglement are absent.

The investigation of entanglement in many-body condensed matter systems is currently a topic of intense activity [13, 14, 15, 16, 17, 18, 10, 1, 19, 3, 8]. In many instances investigations have focussed on the entanglement between individual elements, such as single spins, or the entanglement between two complementary blocks in the ground state of a condensed matter system. The former is generically non-zero only between nearest or next to nearest neighbors [14, 15]; at variance, for complementary blocks, the whole system is in a *pure state* and the von Neumann entropy is a *permissible* measure of the entanglement. In conventional gapless phases, due to the absence of an intrinsic length scale, the von Neumann entropy diverges with the size of the blocks [16, 17, 18]; at variance, our analysis [3, 8] provides for the first time a characterization of the entanglement in gapless regimes of a many body system where a length scale emerges as a result of the presence of a Kondo impurity.

From a more practical viewpoint there is now a huge demand for long range entanglement between individual spins in quantum information theory. For instance, the long range entanglement between individual particles gives the opportunity of implementing teleportation [20] which offers perfect quantum communication between distant parties. Though entanglement in condensed matter systems is typically very short ranged [15], there have been a few other proposals for long distance entanglement; however, they come at a high price. For instance, there are proposals exploiting weak couplings of two distant spins to a spin chain [21, 22], which have very limited thermal stability or very long time-scale of entanglement generation. Otherwise, a dynamics has to be induced by large-scale changes to the Hamiltonian of a system [23].

The paper is organized as follows: In section (2) we review our analysis [3] of the static entanglement properties of the ground state of the Kondo spin chain model using negativity[4] as a true measure of entanglement: there, using only quantum information tools, we are able[3] to determine the spatial extent of the Kondo cloud as well as to provide an ansatz for the ground state in the Kondo regime of the spin chain Kondo model. In section (3) we point out [8] how - only in the Kondo regime of the spin chain Kondo model- a local quench of the last bond of the Kondo spin chain induces a thermally robust high quality long range and distance-independent entanglement between the two individual ending spins of the chain: there, we emphasize how the onset of this long range distance-independent entanglement may be regarded as the footprint of the emergence of the Kondo cloud in the Kondo regime of the spin chain Kondo model. Section (4) is devoted to a short discussion of our results.

2 Entanglement in the Ground State of the Spin Chain Kondo Model

In this section we detail the results of our analysis [3] of the entanglement properties of the ground state of the Hamiltonian described by (1). We show that a true measure of entanglement enables one to use only quantum information tools to determine the Kondo screening length ξ and to provide an ansatz for the ground state of this spin chain in the Kondo regime.

A true measure of entanglement should satisfy a set of postulates - for example, it should be non-increasing under local actions: such a genuine measure does exist for two sub-systems of arbitrary size even when their combined state is mixed, as it happens in Kondo systems. This measure is the *negativity* [4] and it has been successfully used to quantify the entanglement in a harmonic chain [24, 25] and between distant regions of critical systems [26, 27]. For bipartite systems, negativity is

defined as $E = \sum_i |a_i| - 1$, where a_i denote the eigenvalues of the partial transpose of the whole density matrix of the system with respect to one of the two subsets of the given partition and $|\dots|$ is the absolute value [4].

In the following we use DMRG as the numerical tool needed to measure the static entanglement properties observed in the Kondo regime of the spin chain Kondo model.

2.1 The Entanglement Healing Length

To study the entanglement of the ground state we divide- see Fig. 1b - all the spins of the chain in three different groups: the impurity spin, block *A*, which contains the L spins next to the impurity ($L = 0, 1, \dots, N - 1$) and block *B* formed by the remaining $N - L - 1$ spins. We used [3] negativity to fully characterize the entanglement between the impurity and block *B* in both the gapless Kondo and the gapped dimerised regimes.

We determined [3] the size of the block *A* when the entanglement between the impurity and block

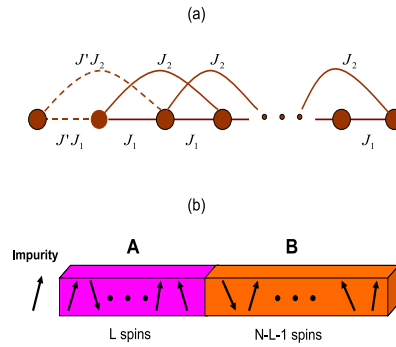


Figure 1: (a) Kondo Spin chain with next nearest neighbor Heisenberg interaction with one impurity at one end. (b) The chain is divided into three parts, an impurity, a block A and a block B . Entanglement is computed between the impurity and block B .

B is almost zero; by this procedure one defines [3] an Entanglement Healing Length (EHL) L^* , i.e. the length of the block A which is maximally entangled with the impurity. It should be emphasized that an EHL may be defined for all spin chains: however, we showed [3] that, only in the gapless Kondo regime of the Kondo spin chain, EHL scales with the strength of the impurity coupling just as the Kondo screening length, ξ , does.

In the gapless regime of the Kondo spin chain, measuring the EHL through negativity [3] yields a genuine quantum information tool to detect the Kondo screening length [1, 6, 7]. In addition we *found* that- in the Kondo regime- entanglement, as quantified by negativity, is a homogeneous function of the two ratios: N/L^* and L/N , where L is the size of the block A , i.e. the block adjacent to the impurity, and N is the length of the whole chain. As a result, the entanglement in the Kondo regime is essentially unchanged if one rescales all the length scales with the EHL L^* . Of course, EHL can be defined also in the gapped dimerised regime but negativity is now a function of the three independent quantities N , L and L^* : i. e., scaling of entanglement with EHL is absent in the gapped dimerised regime [3].

2.2 Numerical Approach: Density Matrix Renormalization Group

The DMRG [28] approach has been used [3] to compute the ground state of the spin chain Kondo model for large chains up to $N = 250$; in order to avoid finite size effects, we took N to be even and, thus, avoided problems arising from accidental degeneracies.

In a DMRG approach the ground state of the system is partitioned in terms of states of a left block, a right block (not to be confused with blocks A and B) and two intermediate spins as shown in Fig. 2a. The states of the intermediate spins are given in the computational ($|\uparrow\rangle, |\downarrow\rangle$) basis, while the states of the both blocks are usually in some non-trivial truncated DMRG basis. In this approach one has several representations for the ground state which vary due to the number of spins in the left (right) block and it is possible to go from one representation to the other by applying pertinent operators on each block.

The main issue in the DMRG is that the dimension of the left (right) block is kept constant and independent of whatever spins are there in that block. To have a fixed dimension for the left (right) block we truncated the Hilbert space so that the amount of entanglement between the two parts of the chain

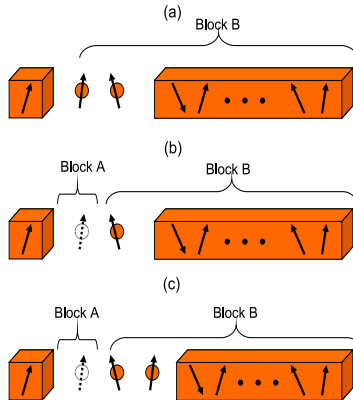


Figure 2: (a) DMRG representation of the state of the chain keeps two intermediate spins in ordinary computational basis and the left and right blocks in a truncated DMRG basis. (b) The intermediate spin next to the impurity is traced out from the density matrix of the chain. This tracing is equivalent to adding the traced out spin to block A. (c) The basis of the right block of DMRG representation is transformed so that a single spin in the left side of the right block is represented in the computational basis while the state of the new right block is given in a DMRG basis.

remains almost unchanged [28]. To improve the precision of our results we swept [3] all representations of the ground state for several times to get the proper basis for the left and the right blocks of all representations. After some sweeps, when the ground state energy converges (we kept states for which the error on the energy is less than 10^{-6}), we paused to compute the entanglement. We took a representation of the ground state in which the left block contains just the single impurity spin and the right block contains $N - 3$ spins: as a result, the single impurity spin is given in the computational basis and this allowed us to compute the negativity later.

From the DMRG state, one should trace out the spins belonging to block A before computing the entanglement between the impurity and block B since it is most convenient to compute the entanglement between the impurity and the block B: due to the entanglement monogamy, this provides an equivalent information about the entanglement of the impurity with the block A. Our tracing procedure started with the density matrix of the ground state of the system in the representation shown in Fig. 2a; at this stage, the number of spins in the block A is zero (no spin has been traced out), all spins except the impurity belong to the block B, and the entanglement between the impurity and the block B is maximal (i.e. $E = 1$). Then, we traced out the intermediate spin next to the impurity as shown in Fig. 2b; this amounts to putting that spin into block A. Finally, as shown in Fig. 2c, we transformed the DMRG basis of the right block so as to put a single spin at the left of the right block in the computational basis, while the state of the new right block is given in a DMRG basis. As a consequence, the resulting density matrix had the exact form of Fig. 2a and we continued the procedure to trace one spin at each step (i.e., put more spins in the block A) and computed the entanglement between the impurity and block B.

2.3 Scaling of Negativity and Ansatz for the Ground State in the Kondo Regime

As evidenced in [3], there is an EHL L^* so that, for $L > L^*$, the entanglement between the impurity and block B is almost zero: L^* provides us with an estimate of the distance for which the impurity is mostly

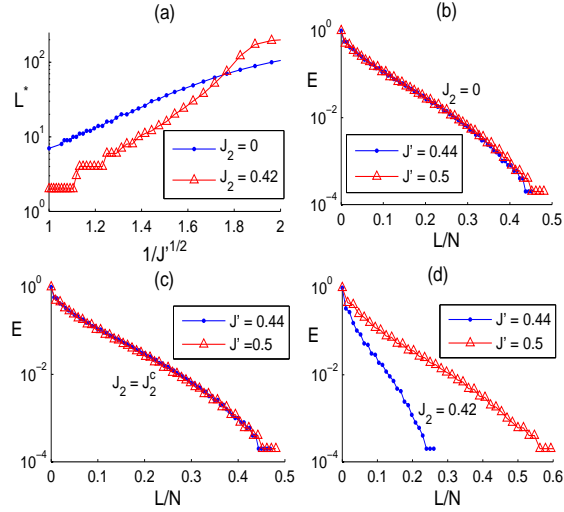


Figure 3: (a) L^* vs. $1/\sqrt{J'}$ for both Kondo ($J_2 = 0$) and dimer regime ($J_2 = 0.42$). (b) Entanglement vs. L/N for fixed $N/L^* = 4$ when $J_2 = 0$. (c) Entanglement vs. L/N for fixed $N/L^* = 4$ at the critical point $J_2 = J_2^c$. (d) Entanglement vs. L/N for fixed $N/L^* = 4$ in the dimer regime ($J_2 = 0.42$).

entangled with the spins contained in block A . For large chains ($N > 200$) in the Kondo regime, one finds that L^* is almost independent of N and depends only on J' . In the Kondo regime, i.e. for $J_2 < J_2^c$, L^* depends on J' just as the Kondo screening length ξ does [10, 1]; for small J' , $L^* \propto e^{\alpha/\sqrt{J'}}$, where α is a constant. We plot L^* as a function of $1/\sqrt{J'}$ in Fig. 3a. In a semi-logarithmic scale, the straight line plot exhibited in the Kondo regime ($J_2 = 0$) shows that L^* may be indeed regarded as the Kondo screening length. Moreover, the nonlinearity of the same plot in the dimer regime ($J_2 = 0.42$), especially for small J' , shows that, in the gapped dimerised regime accessible to the Kondo spin chain model, no exponential dependence on $1/\sqrt{J'}$ holds.

There is [3] also a remarkable scaling of negativity in the Kondo regime. This scaling may be regarded as yet another independent evidence of the fact that L^* is indeed the Kondo length ξ . In general, the entanglement E between the impurity and block B is a function of the three independent variables, J' , L and N which, due to the one to one correspondence between J' and L^* , can be written as $E(L^*, L, N)$. We find that, in the Kondo regime, $E = E(N/L^*, L/N)$. To illustrate this, we fix the ratio N/L^* and plot the entanglement in terms of L/N for different values of J' (or equivalently L^*) for $J_2 = 0$ (Fig. 3b) and for $J_2 = J_2^c$ (Fig. 3c). The complete coincidence of the two plots in Figs. 3b and c shows that, in the Kondo regime, the spin chain can be scaled in size without essentially affecting the entanglement as long as L^* is also scaled. In the dimer regime the entanglement stays a function of three independent variables, i.e. $E = E(L^*, L, N)$, and, as shown in Fig. 3d, the entanglement does not scale with L^* . In our approach, the EHL L^* may be evaluated in both the Kondo and the dimer regime: the scaling behavior, as well as the dependence of L^* on J' , discriminates then between the very different entanglement properties exhibited by the spin chain Kondo model as J_2 crosses J_2^c .

We defined L^* such that there is no entanglement between the impurity and block B when block A is made of L^* spins. Conventional wisdom based on previous renormalization group analysis suggests that, in both regimes, the impurity and the block A of length L^* form a pure entangled state, while block B is also in a pure state. This is indeed approximately true in the dimer regime (exactly true for $J_2 = 0.5$)

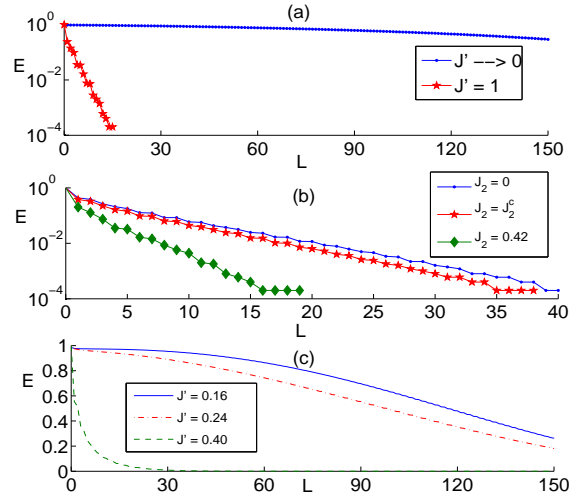


Figure 4: (a) Entanglement vs. L for the two fixed points $J' \rightarrow 0$ and $J' \rightarrow 1$ in the Kondo regime $J_2 = 0$. (b) Exponential decay of entanglement in terms of L in a chain of length $N = 250$ for $J' = 0.6$. (c) Non-exponential decay for small J' in the dimer regime $J_2 = 0.42$.

but it turns out to be dramatically different in the Kondo regime. To check this, we computed the von Neumann entropy of the block B when block A has L^* spins and found it to be non zero. Thus, the blocks A and B are necessarily entangled in the Kondo regime as there is no entanglement between the impurity and B . In fact, after a distance L^* , the impurity is "screened" i.e, the block B feels as if it is part of a conventional gapless chain and has a diverging von Neumann entropy. The Kondo cloud is, then, maximally entangled with the impurity as well as being significantly entangled with block B . Based on the above, a simple ansatz for the ground state $|GS\rangle$ in the Kondo regime has been proposed in [3]; namely, one may conjecture that

$$|GS_I\rangle = \sum_i \alpha_i \frac{|\uparrow\rangle|L_i^\uparrow(J')\rangle - |\downarrow\rangle|L_i^\downarrow(J')\rangle}{\sqrt{2}} \otimes |R_i(J')\rangle, \quad (2)$$

where α_i are constants, $\{ |L_i^\uparrow(J')\rangle, |L_i^\downarrow(J')\rangle \}$ and $\{ |R_i(J')\rangle \}$ are sets of orthogonal states on the cloud and the remaining system, respectively. At the fixed point $J' \rightarrow 0$ all spins except the impurity are included in $|L_i^\uparrow(J')\rangle$ and $|L_i^\downarrow(J')\rangle$. At $J' \rightarrow 1$, very few spins are contained in $|L_i^\uparrow(J')\rangle$ and $|L_i^\downarrow(J')\rangle$ while $\{ |R_i(J')\rangle \}$ represents most of the chain.

For what concerns the mere evaluation of the amount of entanglement as J' is varied, we plot, in Fig. 4a, the negativity as a function of L near by the two fixed points, i.e. $J' \rightarrow 0$ and $J' \rightarrow 1$, accessible in the Kondo regime: as expected, near $J' \rightarrow 0$ (i.e, for large values of the Kondo screening length), the entanglement remains large for rather large values of L while, for $J' \rightarrow 1$ (i.e. for a very small cloud) it decreases rapidly with L . Fig. 4a (semi-logarithmic) shows that, also at the extreme limits $J' \rightarrow 0$ and $J' \rightarrow 1$, the entanglement decays exponentially with L since this a characteristic mark of the entanglement in the Kondo regime. This exponential decay of entanglement is absent in the dimer regime: Fig. 4b shows that, in the gapped dimerised regime, only for rather large J' , the entanglement decays exponentially with L while, for small J' , the entanglement between the impurity and block B decays *slower than an exponential* as a function of L exhibiting even a plateau at short distances. This

latter feature is evidenced in Fig. 4c, and is consistent with the emergence, for small J' , of long range valence bonds between the impurity and far spins as a consequence of the onset of the dimerised ground state [1]. In fact, when J' is small, $J_2 J'$ becomes much less than J_2^c and the impurity forms valence bonds with distant spins, while the other spins, since for them $J_2 > J_2^c$, form a valence bond with their nearest neighbor to preserve the dimerised nature of the ground state: as a result, the impurity shares less entanglement with nearby spins and fulfills its capacity of entanglement forming valence bonds with the more distant spins in the chain.

3 LONG-RANGE DISTANCE-INDEPENDENT ENTANGLEMENT IN THE KONDO REGIME

Entanglement between a single impurity spin and a group of spins- such as the ones inside the Kondo cloud emerging in the Kondo regime accessible to the spin chain Kondo model- cannot be used as a resource for computational tasks since manipulation of many particles is an extremely difficult task. It is much more convenient, instead, to use entanglement between distant individual particles since, due to their localization, one may more easily resort to unitary gates and measurements to control these individual spins. In [8] we proposed a procedure to convert the *useless* entanglement between the impurity and the cloud into the *useful* entanglement between the two ending spins of the Kondo spin chain.

To engineer the long range entanglement between distant individual spins we took [8] the finite Kondo spin chain (1) in its ground state $|GS_I\rangle$ and, then, *pertinently* quenched the coupling at the opposite end of the impurity allowing for the dynamics to develop entanglement. We showed that, in the Kondo regime, the entanglement between the two ending spins oscillates between high peaks with a periodicity determined by J' , while the dynamics is very fast (thereby decoherence hardly gets time to act) and is robust against thermal fluctuations. At variance, in the gapped dimer regime, the dynamics is much slower, qualitatively different and, in finite chains, it still generates some entanglement due to the unavoidable end to end effects, which are drastically tamed if one "cuts off" the impurity from the chain during the dynamics. In the Kondo regime, cutting off the impurity has minimal effect on the final entanglement between the ending spins since, here, the process is induced by the emergence of the Kondo cloud [8].

3.1 Entanglement Oscillations Induced by Local Quench Dynamics in the Kondo Regime

Initially, the system is assumed to be in the ground state $|GS_I\rangle$ of H_I . A minimal quench modifies only the couplings of the N th spin by the amount J' (same as J' in Eq. (1)) so that H_I is changed to

$$\begin{aligned}
 H_F &= J'(J_1 \sigma_1 \cdot \sigma_2 + J_2 \sigma_1 \cdot \sigma_3 + J_1 \sigma_{N-1} \cdot \sigma_N + J_2 \sigma_{N-2} \cdot \sigma_N) \\
 &+ J_1 \sum_{i=2}^{N-2} \sigma_i \cdot \sigma_{i+1} + J_2 \sum_{i=2}^{N-3} \sigma_i \cdot \sigma_{i+2}.
 \end{aligned} \tag{3}$$

Since $|GS_I\rangle$ is not an eigenstate of H_F it evolves as $|\psi(t)\rangle = e^{-iH_F t} |GS_I\rangle$. An entanglement $E(N, t, J')$ between the ending spins emerges as a result of the above evolution.

To compute $E(N, t, J')$, in [8] we computed the reduced density matrix $\rho_{1N}(t) = \text{tr}_{1N} |\psi(t)\rangle \langle \psi(t)|$ of spins 1 and N by tracing out the remaining spins from the state $|\psi(t)\rangle$. Then, we evaluated $E(N, t, J')$ in terms of a measure of entanglement valid for arbitrary mixed states of two qubits called the concurrence [29]. We showed that entanglement took its maximum value E_m at an optimal time t_{opt} and at optimal

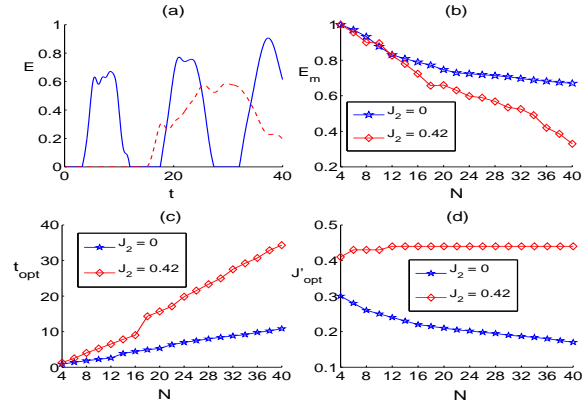


Figure 5: Comparing the Kondo ($J_2 = 0$) and dimer ($J_2 = 0.42$) regimes. (a) Entanglement vs. time for $N = 30$ with $J' = 0.19$ for the Kondo regime (solid line) and $J' = 0.44$ for the dimer regime (dashed line). (b) E_m vs. the length N . (c) t_{opt} vs. N . (d) J'_{opt} vs. length N .

coupling J'_{opt} such that $E_m = E(N, t_{opt}, J'_{opt})$. We evidenced in [8] that J'_{opt} is not a perturbation of J_1 and J_2 . If, as expected from scaling in the Kondo regime [30, 3], the dependence on N and t can be accounted for by a redefinition of J' (equivalently ξ), then t_{opt} and J'_{opt} cannot be independent quantities.

Our numerical analysis showed that, in the Kondo regime, $t_{opt} \propto N$ and that J'_{opt} yields $\xi = N - 2$; since $\xi \propto e^{\alpha/\sqrt{J'}}$ one gets

$$t_{opt} \propto N \propto e^{\alpha/\sqrt{J'_{opt}}}$$

. For our choice of J' , J_1 and J_2 the spin-chain dynamics is not analytically solvable and one has to resort to numerical simulations. Here, for $N > 20$, we used the time-step targeting method, based on the DMRG algorithm introduced in [31]. For $N < 20$, instead, one may resort to exact diagonalization.

We focused only on the first period of the entanglement evolution in both regimes, since both decoherence and numerical errors make it unwise to wait for longer times. Fig. 5(a) shows that fast long-lived (non-decaying) periodic oscillations with a period of $2t_{opt}$ characterize the time evolution in the Kondo regime and that the maximal entanglement is achieved when the impurity coupling J' equals the value J'_{opt} associated to a Kondo cloud of size $\xi = N - 2$ (the Kondo cloud generated by the impurity sitting on the left side touches the other side of the chain); in the dimer regime the dynamics appears more dispersive and not oscillatory for any J' . In Fig. 5(b) we plot the maximum of entanglement, E_m , induced by bond quenching as a function of the length N : though the entanglement decreases as N increases, its value, in the Kondo regime, stays rather high and becomes almost *distance independent* for very long chains; furthermore, as N increases, the entanglement generated in the Kondo regime is significantly bigger than the one in the dimer regime.

Despite its lower value, achieving entanglement in the dimer regime costs more time, as shown in Fig. 5(c). It is also clear from Fig. 5(c) that t_{opt} increases by N linearly. At variance, in the Kondo regime, J'_{opt} slowly decreases as N increases while it stays essentially constant in the dimer regime (Fig. 5(d)). This is commensurate with the expectation that $t_{opt} \propto e^{\alpha/\sqrt{J'_{opt}}}$ in the Kondo regime, while, in the dimer regime, t_{opt} and J'_{opt} are two independent quantities. The plot in Fig. 6a shows the exponential dependence of t_{opt} on $J'_{opt}^{-1/2}$ realized, in the Kondo regime, for long enough chains.

3.2 Probing the Size of the Kondo Cloud through Entanglement's Quench Dynamics

How the dynamics allows to engineer - even for very long chains of size N - high entanglement oscillations between the ending spins of the chain in the Kondo regime? To understand this, one should recall that, in the Kondo regime, the impurity spin forms an effective singlet with all the spins inside the cloud [3] and that, only in this regime, one can always choose J' so that ξ may be made comparable with N ; at variance, in the dimer regime, the impurity in $|GS_I\rangle$ picks out - no matter what the values of J' and N are - only an individual spin in the chain to form a singlet (a valence bond) while the remaining spins form singlets (*local dimers*) with their nearest neighbors [1]. Thus, only in the Kondo regime, one may use the remarkable resource to select - for any N - an initial state $|GS_I\rangle$ which is free from local excitations: in fact, when $\xi = N - 2$ ($J' = J'_{opt}$) there is only a single entity, namely the N th spin, interacting with the impurity-cloud composite. As this situation can always be engineered by choosing, for any N , $J' = J'_{opt}$, this allows for an explanation [8] of the distance-independent entanglement in Fig. 5b. The proposed scenario provides an intuitive grasp on why, only in the Kondo regime, an optimal entanglement between the ending spins may emerge from quench dynamics as the result of the interplay between very few states. At variance, in the dimer regime, the energy released by quenching is dispersed over the variety of different quantum modes associated to the local dimers and no significant long range entanglement may then be engineered.

To provide a more quantitative analysis, one may expand $|\psi(t)\rangle$ in terms of eigenvectors of H_F . By exact diagonalization (up to $N = 20$), one finds that, in the Kondo regime, only two eigenstates of H_F (the ground state $|E_1\rangle$ and one excited state $|E_2\rangle$) predominantly contribute to the dynamics:

$$\begin{aligned} |E_1\rangle &= \alpha_1 |\psi^-\rangle_{1N} |\phi^-\rangle_b + \beta_1 (|00\rangle_{1N} |\phi^{00}\rangle_b \\ &\quad + |11\rangle_{1N} |\phi^{11}\rangle_b - |\psi^+\rangle |\phi^+\rangle_b) \\ |E_2\rangle &= \alpha_2 |\psi^-\rangle_{1N} |\phi^-\rangle_b - \beta_2 (|00\rangle_{1N} |\phi^{00}\rangle_b \\ &\quad + |11\rangle_{1N} |\phi^{11}\rangle_b - |\psi^+\rangle |\phi^+\rangle_b). \end{aligned} \quad (4)$$

In Eq. (4) the first and the last spin are projected onto the singlet ($|\psi^-\rangle$) and the triplets ($|00\rangle, |11\rangle$ and $|\psi^+\rangle$) while the states of all spins in the body of the chain have been specified by the index b . After a time t the state evolves as

$$|\psi(t)\rangle = \langle E_1 | GS_I \rangle |E_1\rangle + e^{-i\Delta E t} \langle E_2 | GS_I \rangle |E_2\rangle + \dots, \quad (5)$$

where, ΔE is the energy separation between the two levels. One defines $t = t_{opt}$ as the time for which the contribution of $|\psi^-\rangle_{1N} |\phi^-\rangle_b$ is most enhanced in $|\psi(t)\rangle$ due to a *constructive interference*.

The condition for the onset of constructive interference is

$$|\langle E_1 | GS_I \rangle \beta_1| \approx |\langle E_2 | GS_I \rangle \beta_2|, \quad (6)$$

so that terms other than $|\psi^-\rangle_{1N} |\phi^-\rangle_b$ in $|\psi(t)\rangle$ do not contribute at $t = t_{opt}$. When $J' \rightarrow 1$ (very small cloud) then $|\langle E_1 | GS_I \rangle| \approx 1$ while $|\langle E_2 | GS_I \rangle| \approx 0$ as the ground state is hardly changed on quench: thus, constructive interference between $|E_1\rangle$ and $|E_2\rangle$ it is impossible. The condition of Eq. (6) cannot be satisfied also when $J' \rightarrow 0$, since one has now that $\beta_1 \approx 0$ and $\beta_2 \approx 1$ (the end spins form a singlet and triplet with each other in $|E_1\rangle$ and $|E_2\rangle$ respectively [21]). Thus, only for intermediate J' entanglement may peak. When $J' > J_{opt}$ ($\xi < N - 2$)- and particularly for $\xi < N/2$ - the entanglement between the ending spins is frustrated by the existence of local excitations whose number increases as the size of the cloud gets smaller. In addition, when $J' < J_{opt}$ ($\xi > N - 2$), the Kondo cloud overtakes the chain and the N th spin is already *included in the cloud* and its tendency is to screen the original impurity as

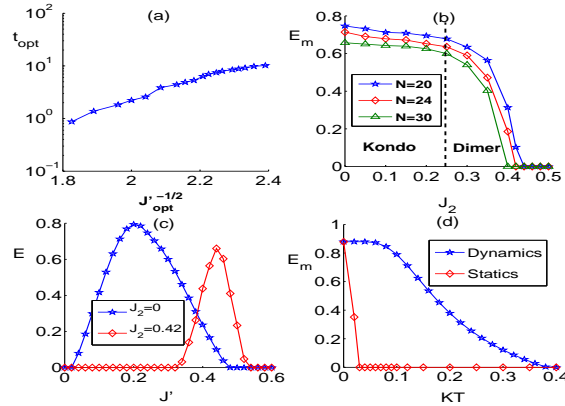


Figure 6: (a) t_{opt} vs. $1/\sqrt{J'_{opt}}$ in the Kondo regime. (b) E_m at $t \propto 1/J'_{opt}$ vs. J_2 for chains of different lengths. (c) Entanglement attained at t_{opt} vs. J' for Kondo and dimer regimes for $N = 20$. (d) E_m vs. temperature after bond quenching (blue line) and induced by (static) weak coupling with the rest of the chain (red line) for a chain of $N = 10$.

in $|\psi^-\rangle_{1N}|\phi^-\rangle_b$ rather than to pair with it to form a spin one (as in the last three terms of $|E_1\rangle$). This makes β_1 quite small, and it becomes smaller as the cloud overtakes the chain and again the condition of Eq. (6) cannot be fulfilled. Consequently, the optimal situation is realized when $J' = J'_{opt}$ ($\xi = N - 2$), i.e just before the cloud overtakes the chain. Thus, only in the Kondo regime, one can convert-for any N - the *useless entanglement* between the impurity spin and the Kondo cloud into a *usable entanglement* between the ending spins of the chain. The emerging long distance entanglement analyzed in this paper is, indeed, a genuine footprint of the presence of the Kondo cloud in $|GS_I\rangle$ (Fig. 7(a)).

In Fig. 6b we plot- for both regimes- the entanglement reached after waiting for a time interval of the order of $1/J'_{opt}$. One notices that, for $J_2 > J_2^c$, the entanglement peak decreases sensibly and goes to zero rather soon. The plot of the maximal entanglement vs. J' is given in Fig. 6c: here one sees that, in the Kondo regime, the entanglement rises from zero already at very small values of J' . This is expected since, in the Kondo regime, to a small J' is associated a large cloud containing the impurity sitting on the left side.

The essential role of the Kondo cloud in the entanglement generation is further probed if one let evolve the ground state $|GS_I\rangle$ with a doubly quenched Hamiltonian obtained from (3) by isolating (i.e., putting $J' = 0$) the left hand side impurity while keeping fixed to J'_{opt} the bond connected to the last spin (see Fig. 7b). This forbids the dynamical build up of that “portion” of the total entanglement which is only due to end to end effects. In Fig. 8 we have plotted the E_m vs. N after double quenching in both regimes. Fig. 8 shows that entanglement in the dimer phase collapses already when $N > 12$ while it stays *unexpectedly* high - and almost independent on N - in the Kondo regime; the existing entanglement of the Kondo cloud with the impurity [3] is dynamically swapped over to the last spin.

3.3 Thermal Robustness of the Kondo Cloud Mediated Entanglement

Note that a long distance singlet between the end spins may be realized in a ground state when those spins are very weakly coupled ($J' = \varepsilon/\sqrt{N} \ll 1/\sqrt{N}$) to a spin chain [21]. This static approach to generate entanglement relies on couplings which are so weak that they can merely be regarded as perturbations. Such entanglement is not robust against thermal fluctuations due to the smallness of the gap

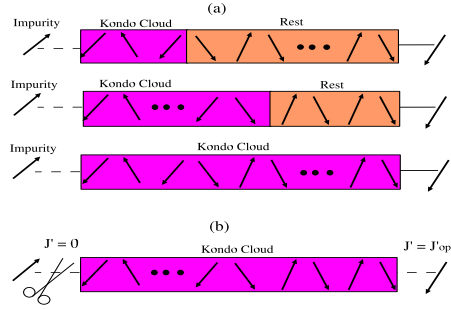


Figure 7: (a) Different $|GS_I\rangle$ for entanglement generation through quench dynamics. Top: The ground states with $\xi < N/2$ (no entanglement). Middle: $N/2 < \xi < N-2$ (some entanglement). Bottom: $\xi = N-2$ (optimal entanglement). (b) Decoupling the impurity from the chain.

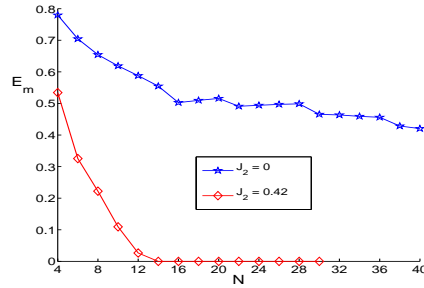


Figure 8: E_m vs. N after decoupling the first impurity.

($\propto J'^2 = \varepsilon^2/N$) between the ground state and a triplet state between the end spins. On the other hand our approach enables to generate entanglement dynamically even for J' as high as $J'_{opt} \approx 1/(\log N)^2$. Even when temperature is increased, the entanglement is not seriously disrupted till $K_B T$ exceeds the Kondo temperature ($\propto 1/\xi = 1/(N-2)$) after which the Kondo cloud does not form. As a result, while in the dynamical approach $K_B T < 1/(N-2)$, in the static approach one has $K_B T < \varepsilon^2/N$: thus, the long distance entanglement generated through the dynamical approach is thermally more stable. For instance, for $\varepsilon \sim 10^{-1}$, our dynamical approach is robust for temperatures 100 times higher than those required for the static approach. In Fig. 6d, we plot E_m - as obtained in both approaches- vs. temperature for $N = 10$. In the static approach, the ground state is replaced by the thermal state, whereas in our dynamic approach it is the initial state which is taken to be the relevant thermal state. We ignore thermalization and relaxation during dynamics since the dynamical time scale, set by t_{opt} , is fast enough (this is also an advantage over slow dynamical schemes with weak couplings [22]).

We should also point out some systems where the Kondo cloud mediated long distance entanglement may be observed such as spin chains in ion traps [32], with trapped electrons [33], in chains of P donors in Si [34] and Josephson chains with impurities [35].

4 Summary

To summarize, we reviewed our analysis [3] of the ground state entanglement of the Kondo spin chain model from the viewpoint of a genuine entanglement measure, namely the negativity. This readily showed that the impurity spin is indeed maximally entangled with the Kondo cloud; we provided an independent method to determine the Kondo screening length together with a characterization of the ground state of the Kondo spin chain in the Kondo regime. We proposed an improved DMRG approach enabling to account for the entanglement between the impurity and a block of spins located at the other side of the chain for different lengths of the block. We defined an Entanglement Healing Length EHL and showed that, in the Kondo regime, the EHL L^* scales with the impurity coupling J' just as the Kondo length does. Finally, our approach showed that, in the Kondo regime, the entanglement scales exponentially with L/L^* and that, in the gapped dimer regime, though it is still possible to define an EHL, the impurity-block entanglement is usually smaller and has no characteristic length scale.

We have also shown that substantial long range distance independent entanglement can be engineered by a non-perturbative quenching of a single bond in the Kondo regime- and only here!- of a Kondo spin chain. This is the first example where a *minimal local* action on a spin chain dynamically creates long range entanglement. In contrast to all known schemes for entanglement between individual spins in spin chains, here the entanglement attains a constant value for long chains rather than decaying with distance. This behavior arises since, in the Kondo regime, one may always select the initial state so as to fulfill the condition $\xi = N - 2$. As the coupling is non-perturbative in strength ($J'_{opt} \approx 1/(\log N)^2$), the entanglement generation is both fast and thermally robust. The long distance entanglement mediated by the cloud and the periodic dynamics, provides a clear signature of the existence of the Kondo cloud in a quantum system with impurities. These features are not seen when the Kondo cloud is absent, e.g., in the gapped dimer regime and- more remarkably- in other conventional gapless systems.

Acknowledgements– AB and SB are supported by the EPSRC, QIP IRC (GR/S82176/01), the Royal Society and the Wolfson Foundation. PS was partly supported by the ESF Network INSTANS.

References

- [1] E. S. Sorensen, M. S. Chang, N. Laflorencie and I. Affleck, J. Stat. Mech., P08003 (2007); E. S. Sorensen, M. S. Chang, N. Laflorencie and I. Affleck, J. Stat. Mech. L01001 (2007).
- [2] I. Affleck, Lecture Notes, Les Houches 2008, arXiv:0809.3474.
- [3] A. Bayat, P. Sodano, S. Bose, Phys. Rev. B **81**, 064429 (2010).
- [4] G. Vidal, R. F. Werner, Phys. Rev. A **65**, 032314 (2002); M.B. Plenio, Phys. Rev. Lett. **95**, 090503 (2005).
- [5] A. Hewson, *The Kondo Model to Heavy Fermions*, Cambridge (1997).
- [6] H. Frahm and A. A. Zvyagin, J. Cond. Matt. **9**, 9939 (1997).
- [7] R. G. Pereira, N. Laflorencie, I. Affleck and B. I. Halperin, Phys. Rev. B **77**, 125327 (2008).
- [8] P. Sodano, A. Bayat and S. Bose, Phys. Rev. B **81**, 100412(R) (2010).
- [9] N. Laflorencie, E. S. Sorensen and I. Affleck, J. Stat. Mech. P02007 (2008).
- [10] N. Laflorencie, E. S. Sorensen, M. S. Chang and I. Affleck, Phys. Rev. Lett. **96**, 100603 (2006).
- [11] C.K. Majumdar and D.K. Ghosh, J. Phys. C: Solid State Phys. **3**, 911 (1969).
- [12] U. Schollwock, Th. Jolicoeur and T. Garel, Phys. Rev. B **53**, 3304 (1996).
- [13] L. Amico, R. Fazio, A. Osterloh, V. Vedral, Rev. Mod. Phys. **80**, 517 (2008).
- [14] M. C. Arnesen, S. Bose and V. Vedral, Phys. Rev. Lett. **87**, 017901 (2001).

- [15] A. Osterloh, L. Amico, G. Falci, R. Fazio, Nature **416**, 608-610 (2002); T. J. Osborne and M. A. Nielsen, Phys. Rev. A **66**, 032110 (2002).
- [16] G. Vidal, J. I. Latorre, E. Rico, and A. Kitaev, Phys. Rev. Lett **90**, 227902 (2003).
- [17] B. Q. Jin and V. E. Korepin, J. Stat. Phys. **116**, 79-95 (2004).
- [18] P. Calabrese, J. Cardy, J. Stat. Mech., P06002 (2004).
- [19] K. Le Hur, P. Doucet-Beaupre and W. Hofstetter, Phys. Rev. Lett. **99**, 126801 (2007); K. Le Hur, Ann. of Phys. **323**, 2208 (2008).
- [20] C. H. Bennett, *et al.*, Phys. Rev. Lett. **70**, 1895, (1993).
- [21] L. Campos Venuti, C. Degli Esposti Boschi and M. Roncaglia, Phys. Rev. Lett. **96**, 247206 (2006); L. Campos Venuti, S. M. Giampaolo, F. Illuminati, P. Zanardi, Phys.Rev.A **76**, 052328 (2007).
- [22] L. Campos Venuti, C. Degli Esposti Boschi and M. Roncaglia, Phys. Rev. Lett. **99**, 060401 (2007); M. J. Hartmann, M. E. Reuter, M. B. Plenio, New J. Phys. **8**, 94 (2006); Y. Li, *et. al.*, Phys. Rev. A **71**, 022301 (2005); A. Wojcik, *et. al.*, Phys. Rev. A **72**, 034303 (2005).
- [23] H. Wichterich, S. Bose, Phys. Rev. A **79**, 060302(R) (2009); Fernando Galve, *et. al.*, Phys. Rev. A **79**, 032332 (2009).
- [24] K. Audenaert, J. Eisert, M. B. Plenio, R. F. Werner, Phys. Rev. A **66**, 042327 (2002).
- [25] J. Kofler, J. Kofler, V. Vedral, M. S. Kim and Caslav Brukner, Phys. Rev. A **73**, 052107 (2006).
- [26] H. Wichterich, J. Molina-Vilaplana, S. Bose, Phys. Rev. A **80**, 010304(R) (2009).
- [27] S. Marcovitch, A. Retzker, M. B. Plenio, B. Reznik, Phys. Rev. A **80**, 012325 (2009).
- [28] S. R. White, Phys. Rev. Lett. **69**, 2863 (1992); S. R. White, Phys. Rev. B **48**, 10345 (1993).
- [29] W.K. Wootters, Phys. Rev. Lett. **80**, 2245 (1998).
- [30] E. S. Sorensen and I. Affleck, Phys. Rev. B **53**, 9153 (1996).
- [31] A. E. Feiguin and S. R. White, Phys. Rev. B **72**, 020404 (2005).
- [32] D. Porras, J. I. Cirac, Phys. Rev. Lett. **92**, 207901 (2004); F. Mintert and C. Wunderlich, Phys. Rev. Lett. **87**, 257904 (2001); A. Friedenauer, *et. al.*, Nature Physics **4**, 757 (2008).
- [33] G. Ciaramicoli, I. Marzoli, and P. Tombesi, Phys. Rev. A **75**, 032348 (2007).
- [34] B. E. Kane, Nature **393**, 133 (1998).
- [35] D. Giuliano and P. Sodano, Nucl. Phys. B **811**, 395(2009).